Expression of RAD21 immunoreactivity in myenteric neurons of the human and mouse small intestine

HHS Public Access

Author manuscript

Neurogastroenterol Motil. Author manuscript; available in PMC 2019 September 01.

Published in final edited form as:

Neurogastroenterol Motil. 2018 September ; 30(9): e13429. doi:10.1111/nmo.13429.

Expression of RAD21 Immunoreactivity in Myenteric Neurons of the Human and Mouse Small Intestine

Francesca Bianco[1,2], **Seth T. Eisenman**[3,4], **Maria Gabriela Colmenares Aguilar**[3,4], **Elena Bonora**[1], **Paolo Clavenzani**[2], **David R. Linden**[3,4], **Roberto De Giorgio**[5], **Gianrico Farrugia**[3,4], and **Simon J. Gibbons**[3,4]

[1]Dept. of Medical and Surgical Sciences (DIMEC), University of Bologna, Bologna, Italy

[2]Dept. of Veterinary Medical Sciences (DIMEVET), University of Bologna, Bologna, Italy

[3]Enteric NeuroScience Program, Mayo Clinic, Rochester, MN, USA

[4]Dept. of Physiology and Biomedical Engineering, Mayo Clinic, Rochester, MN, USA

[5]Dept. of Medical Sciences, Nuovo Arcispedale S.Anna, University of Ferrara, Ferrara, Italy

Abstract

Background: RAD21 is a double-strand-break repair protein and component of the cohesin complex with key roles in cellular functions. A RAD21 loss-of-function mutation was found in cases of chronic intestinal pseudo-obstruction (CIPO) with associated enteric neuronal loss. Analysis of RAD21 expression in the enteric nervous system is lacking, thus we aimed to characterize RAD21 immunoreactivity (IR) in myenteric ganglia.

Methods: Double labeling immunofluorescence in mouse and human jejunum was used to determine co-localization of RAD21 with HuC/D, PGP9.5, neuronal nitric oxide synthase (nNOS), neuropeptide Y (NPY), choline acetyl transferase (ChAT), Kit, platelet-derived growth factor receptor-α (PDGFRα) and glial fibrillary acid protein (GFAP) IRs.

Results: A subset of PGP9.5- and HuC/D-IR neuronal cell bodies and nerve fibers in the myenteric plexus of human and mouse small intestine also displayed cytoplasmic RAD21-IR. Cytoplasmic RAD21-IR was found in 43% of HuC/D-IR neurons in adult and neonatal mice but did not co-localize with nNOS. A subset of ChAT-positive neurons had cytoplasmic RAD21-IR. Punctate RAD21-IR was restricted to the nucleus in most cell types consistent with labeling of the cohesin complex. Cytoplasmic RAD21-IR was not detected in interstitial cells of Cajal, fibroblast-

Corresponding author: Simon J Gibbons, PhD, Enteric Neuroscience Program and Department of Physiology and Biomedical Engineering, Mayo Clinic, Rochester, MN, USA, gibbons.simon@mayo.edu, Telephone: 507 284 4695, Fax: 507 284 0266.

Disclosures:

RDeG has participated as a consultant for Shire, Sucampo, Coloplast, Kyowa Kirin International, Takeda and received grant support from Shire and Takeda.

The other authors declare no conflict of interest.

Authors contributions:

FB, SJG conceived the study, performed data analysis and wrote the manuscript; FB, STE, MGCA performed immunostaining, whole mounts and primary culture preparations; SJG and GF provided the clinical cases and tissue biopsies; SJG, GF, RDeG and EB obtained funding SJG, GF, DRL, RDeG, EB and PC, performed critical revision of the manuscript. All authors read the final version of the paper and had complete access to the data that support this publication.

like cells or glia. Subsets of neurons in primary culture exhibited cytoplasmic RAD21-IR. Suppression of RAD21 expression by shRNA knock-down abolished RAD21-IR in cultured neurons.

Conclusions: Our data showing cytoplasmic RAD21 expression in enteric neurons provide a basis towards understanding how mutations of this gene may contribute to altered neuronal function/survival thus leading to gut-motor abnormalities.

Graphical Abstract

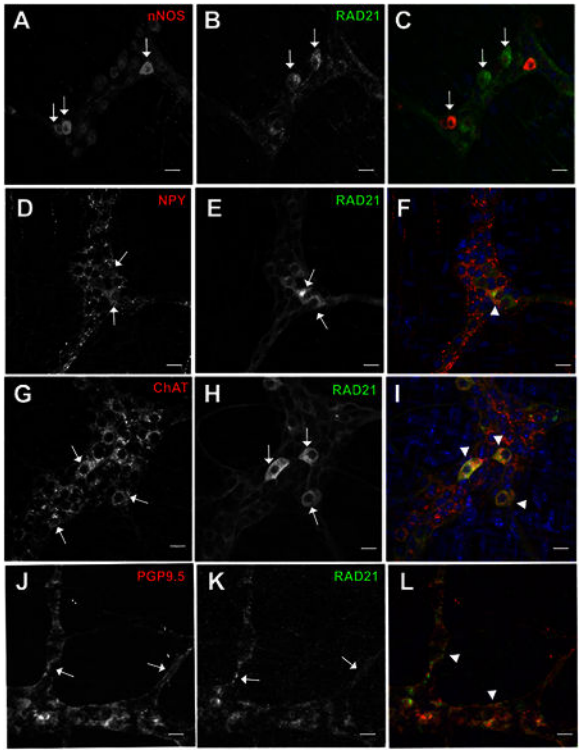

RAD21 is a double-strand-break repair protein and a component of the cohesin complex. A RAD21 loss-of-function mutation was found in cases of chronic intestinal pseudo-obstruction with associated enteric neuronal loss. We found RAD21 immunolabeling in the cytoplasm of cholinergic but not nitrergic myenteric neurons, consistent with differential roles of RAD21 in neuronal function/survival and possibly gut-motor abnormalities.

Keywords

chronic intestinal pseudo-obstruction; enteric neurons; immunofluorescence

INTRODUCTION

RAD21 is a transcription factor and a key central component of the multi-protein cohesin complex,[1] which functions to protect chromosome separation during the metaphase–anaphase transition of mitosis.[2] RAD21 is ubiquitously expressed[3] and its critical role was indicated by the lethal early embryonic phenotype in RAD21 knockout mice.[4] Studying a

familial cluster of chronic intestinal pseudo-obstruction (CIPO), we have recently demonstrated a novel loss-of-function mutation in RAD21 which was associated with enteric neuropathy and severe gut dysmotility, in affected family members. The CIPO-causing RAD21 mutation was found to alter the expression of related genes, including RUNX1 and APOB. Indeed, APOB48, the gut-specific isoform of APOB, was overexpressed in sera of patients with CIPO carrying the RAD21 mutation.[5]

CIPO is a rare and intractable chronic digestive disease in which clinical symptoms of intestinal obstruction appear without mechanical cause.[6,7] CIPO can result from derangement affecting the integrity of a variety of regulatory cells/tissues, i.e. smooth muscle cells (effectors of contractility / relaxation), the interstitial cells of Cajal (ICC) (pace-makers of gut motility and regulators of neuronal input to smooth muscle cells), and neurons (both extrinsic and enteric nervous system).[6] Specifically, the RAD21 loss-of-function mutation was associated with a markedly reduced number of enteric neurons, thus implying a neurogenic origin of the gut dysmotility reported in the affected family.[5,8] The clinical evidence that the small bowel is most affected in CIPO, provided the background to our set of experiments focusing on RAD21 expression in the small bowel. The distribution of RAD21 in the enteric nervous system, the intrinsic neural network controlling gastrointestinal (GI) physiology and homeostasis,[9,10] is unknown. The enteric nervous system contains different functionally distinct neuronal subclasses, e.g. motor neurons – either excitatory or inhibitory, interneurons and intrinsic primary afferent neurons, which can be identified according to their neurochemical coding.[10] Inhibitory motor neurons are immunohistochemically identified by the presence of the neuronal isoform of the enzyme nitric oxide synthase (nNOS) leading to nitric oxide synthesis, whereas most excitatory motor neurons are immunohistochemically identified by choline acetyltransferase (ChAT) (the acetylcholine synthesizing enzyme) or via detection of peptides of the tachykinin family (e.g., substance P or neurokinin A). In addition to these two major subclasses of enteric neurons, a variety of secondary neurotransmitters or modulators, e.g. neuropeptide Y (NPY), can be co-synthesized, stored and released by other enteric neuronal subsets, depending on their localization throughout the GI tract and the mammalian species considered.[11] The present study was designed to investigate whether RAD21 expressed in a subset of myenteric neurons in human and mouse small intestine. Furthermore, in order to establish whether RAD21 is influenced by age-dependent mechanisms, we compared the RAD21 expression in myenteric neurons of the small intestine from adult vs. young mice. Our findings clearly demonstrated enrichment of RAD21-IR in the cell bodies and nerve fibers of a subset of myenteric cholinergic, but not nitrergic, neurons in tissues and in primary culture using two different primary antibodies. Silencing (shRNA) of RAD21 expression confirmed specificity of RAD21-IR. This work was previously presented in abstract form[12].

MATERIALS AND METHODS

All authors have access to the study data and have reviewed and approved the final manuscript.

Immunohistochemistry

Single and double labeling immunofluorescence for RAD21 was done using two specific, commercially available rabbit and goat polyclonal antibodies (Abcam, Cambridge MA and Santa Cruz, Dallas TX, respectively see Table 1 for details) directed to RAD21 protein according to previously validated protocols.[13] Normal human small bowel (jejunum) was obtained from n=3 (2F, age: 35–48 yrs) patients undergoing surgery for gastrointestinal cancers or having bariatric surgery at Mayo Clinic, MN, USA. The use of human tissue for research was approved by the Institutional Review Board of Mayo Clinic. Small bowel whole mount preparations from adult (n= 4) and young (n= 3) BALB/c (Harlan Sprague-Dawley, IN, USA) mice were processed for RAD21 immunolabeling (Abcam antibody at the same dilution used for human tissues, Table 1). Mouse brain fixed in 4% paraformaldehyde was cut into 50 μm sections and processed as floating sections in the same manner as whole mount preparations from the small intestine. Mice were killed by CO_2 inhalation and all experiments were approved by the Institutional Animal Care and Use Committee of the Mayo Clinic. Immersion-fixed (4% paraformaldehyde) human tissues (10 μm thick) and acetone-fixed mouse whole mounts were incubated overnight at 4°C with rabbit RAD21 primary antibody as well as with a number of antibodies to a variety of neuronal, neurochemical, glial, and ICC markers (for details see Table 1). After washing, sections and whole mounts were incubated with donkey fluorescein- and rhodamine-conjugated anti-rabbit secondary antibodies as well as secondary antibodies to the previously mentioned markers (Jackson ImmunoResearch West Grove PA, See Table 1 for details) for about 2 h at room temperature. Sections and whole mounts were thoroughly washed in 0.1 M phosphate buffered saline (PBS) and mounted in SlowFade® Gold Antifade Reagent with 4, 6-diamidino-phenylindole,dihydrochloride (DAPI) (Invitrogen, CA, USA), as a nuclear counterstain. Specificity tests to ensure that there was no cross reaction among secondary antibodies included omission and substitution of primary or secondary antibodies. Secondary antibodies directed against IgG from a different species were used to control for the specificity of secondary antibodies in doubly labeled tissues.

Primary cultures from mouse jejunum

Primary cultures were obtained by enzymatic dissociation of mouse jejunum from neonatal mice (post-natal day 3) based on a previously described protocol.[14] Utilizing a collagenase-based dissociation cocktail, tissues were dissociated and then plated on a feeder layer of fibroblasts expressing the membrane bound m248 form of Kit ligand (steel factor). Cells were grown in M199 media (Invitrogen) with 1% antibiotic/antimycotic mixture (Gibco). Primary cells were allowed to attach and recover for 24 hours before treatment. Living, single cells (150,000 each coverslip) were plated in a 12 -well plate with 1 ml of media M199 (Thermo Fisher, Waltham, MA, USA). Primary cultures were maintained at 37°C, 20% O_2, 5%CO_2 in M199 supplemented with glucose (4.5 g l^{-1}, Sigma), antibiotic/antimycotic mixture (penicillin G sodium, 200 i.u. ml^{-1}; streptomycin sulphate, 200 μg ml^{-1}; amphotericin B, 0.5 μg ml^{-1}; Thermo Fisher). Cultures were immunolabeled for RAD21, nNOS, ChAT HuC/D and PGP9.5 antibodies (see Table 1). Nuclei were counterstained with DAPI (Molecular Probes, Eugene, OR, USA).

shRNA lentiviral particles transduction in primary cell cultures

Primary cultures from 3 day old mice were exposed to shRNA lentiviral particles to knock down expression of RAD21 as follows: 50% of the culture medium was replaced with conditioned media and each experimental condition was run in duplicate. Cells were transduced for 24 h by adding to the culture medium 2 μg/mL polybrene (Santa Cruz) and viral particles. Cultures were treated with non-targeting (NT) and shRNA RAD21 (n = 3) lentiviral transduction particles (Santa Cruz shRNA lentiviral transduction particles) with a multiplicity of infection (MOI) of 1 based on the confluence of the mixed cell culture being 50–70% at the time of treatment. For the next 5 days, cultures were washed and fresh culture medium was added daily. After day 1 and 5, cultures were used for RAD21 immunolabeling.

Confocal microscopy

Images of immunolabeling were collected using an Olympus FV1000 laser scanning confocal microscope. Confocal images were collected with ×60 1.2-NA or ×20 0.95-NA water objectives. Quantitative analysis counted the numbers of immunolabeled neurons using Olympus Fluoview Ver.2.1c viewer program. Neurons were counted from (635×635) μm^2 fields per tissue. All images were prepared for individual figures using Adobe Photoshop CS. No 3D reconstructions, deconvolution, surface or volume rendering, or gamma adjustments were performed.

Statistics

Data are expressed as means ± SEM. Statistical significance was determined by GraphPad Prism using Student's t-test. P values of less than 0.05 were taken as statistically significant. The 'N' value identifies the animal count.

RESULTS

Extranuclear RAD21 immunoreactivity in human myenteric neurons from the small intestine

RAD21-IR was present in cell bodies and nerve fibers of a subset of human small intestinal enteric neurons identified by HuC/D-IR (Figure 1 A-C) and PGP9.5 (Figure 1 D-F) respectively. RAD21-IR was not detected in nNOS-IR inhibitory neurons (Figure 1 G-I, arrow). RAD21-IR colocalized with ChAT in some neurons (Figure 1 J-L, arrowhead). Discrete punctate labeling, consistent with labeling of the cohesion complex, was observed in most cells (inset Figure 1I). To further characterize this labelling pattern, we used mouse small intestine.

Extranuclear RAD21 immunoreactivity in mouse myenteric neurons from the small intestine

The extra-nuclear labeling pattern of RAD21-IR was confirmed using two different primary antibodies raised against different epitopes in two different species. Rabbit (Figure 2A) and goat (Figure 2B) anti-RAD21 antibodies labeled most brightly in the same neuronal structures (Figure 2C) in thin sections from mouse jejunum. The goat anti-RAD21 antibody (Figure 2B) gave the clearest neuronal signal, whereas, although neuronal cell bodies were

most bright with the rabbit anti-RAD21 antibody, some background labeling in the muscle layers was evident (Figure 2A). Additional controls were performed to ensure specificity for RAD21 with regard to each primary antibody. Pre-adsorption of antibody with specific blocking peptide abolished the signal suggesting specificity of antibody used (Figure 2D-F). Furthermore, no IR was observed when the tissue preparations were incubated with only secondary antibody, demonstrating that there was no non-specific labeling by the secondary antibody (data not shown).

RAD21-IR is detected in the cytoplasm of a subset of HuC/D-positive myenteric neurons of adult and young mice

Whole mount analyses were conducted in order to determine the mapping of RAD21 expression in adult and young mouse enteric nervous system. We performed RAD21 and HuC/D double labeling immunohistochemical analysis of adult BALB/C mice (n=4; age range: 4–8 weeks). In whole mounts of adult mouse small intestine, RAD21-IR was present in 42.5% of HuC/D positive myenteric neurons. Notably, RAD21-IR was detected in the cytoplasm of a subset of neurons (arrowheads in Figure 3A). Overall, there were 61.56±0.9 RAD21 and 144.7±4.1 HuC/D-positive neurons/field (6 fields per preparation; each field measured 635×635 μm^2, n = 4 mice ($P< 0.05$, Figure 3B).

To determine if RAD21 expression in the cytoplasm of enteric neurons is age dependent, we analyzed the expression of RAD21 in young mice (age range: 4 to 10 days old) (Figure 3C). Similar to adult mice, in young mice RAD21-IR was present in 43% of HuC/D positive myenteric neurons. Specifically, 79.56±4.5 RAD21 and 185.0±4.0 HuC/D-positive neurons/field (6 fields per preparation; each field measured 635×635 μm^2) (n= 3, $P< 0.05$, t-test) (Figure 3D, $P< 0.05$ compared to adult mice).

Chemical coding of RAD21-IR neurons

Co-labeling with several antibodies were used to clarify the neurotransmitters expressed in RAD21 positive neurons (Table 1). RAD21-IR did not co-localize with nNOS (Figure 4A-C arrows). We also detected RAD21-IR cells that were positive for the neuronal peptide NPY in whole mount preparations (Figure 4D-F). RAD21-IR was present in a subset of neurons that expressed ChAT (Figures 4G-I arrowhead). Co-labeling of preparations with PGP9.5 demonstrated RAD21-IR in neuronal fibers (Figure 4J-L).

RAD21 did not colocalize with Kit (ICC), PDGFRα or enteric glia (GFAP) in mice

Cytoplasmic RAD21-IR was not detected in ICC (Figure 5A-D) or PDGFRα-IR fibroblast-like cells (Figure 5E-H) in mouse whole mount preparations. RAD21-IR also did not overlap with glial fibrillary acid protein (GFAP)-IR (Figure 5I-L) in mouse jejunal myenteric ganglia indicating that RAD21 is not expressed in the cell bodies of enteric glia.

RAD21-IR was not detected in the cytoplasm of central cholinergic neurons

To determine whether the cytoplasmic RAD21 immunolabeling pattern was specific to cholinergic myenteric neurons or a feature of cholinergic neurons in general, we investigated the distribution of RAD21-IR in the basal forebrain of a mouse, where central cholinergic neurons are located.[15] in brain sections doubly labeled for ChAT and RAD21, approximately

50% of all cholinergic neurons in this region of the brain showed RAD21-immunolabeling, which was restricted to the nuclear region (Figure 5M-O). Thus, the RAD21 cytoplasmic labeling pattern appears to be a feature of cholinergic myenteric, rather than central, neurons.

RAD21 expression in primary cultures from neonatal mouse jejunum

Primary cultures from mouse small intestinal muscularis propria that contains myenteric neurons showed RAD21-IR similar to that observed in tissues. RAD21-IR was observed in the cell bodies and nerve fibers of a subset of enteric neurons that were identified by PGP9.5 (Figure 6A-D). RAD21-IR was also detected outside the nucleus of a subset of ChAT-IR neurons (Figure 6E-H), but not in nNOS-IR inhibitory neurons (Figure 6I-L).

We next used a shRNA lentiviral approach to knock down RAD21 in primary cultures. We first determined if we could maintain intact RAD21 expression in 5-day-old primary cultures. We prepared primary cultures from mouse jejunum (4 days old), grew these cultures for up to 5 days and performed an immunohistochemistry analysis for RAD21 (Figure 7A-E). We observed no significant changes in RAD21-IR when labelled after 5 days in primary culture (Figure 7F) compared to 1 day in primary culture (Figure 7B). We next optimized the knock down of RAD21 using Santa Cruz transduction shRNA-RAD21. RAD21-IR was abolished in shRNA treated cultures grown for up to 5 days confirming the specificity of the RAD21 antibody and that the signal represented RAD21 protein expression in a subset of enteric neurons (Figure 7J).

DISCUSSION

In the present study we demonstrated that RAD21-IR is expressed in cell bodies and processes of a subset of neurons of the adult human and mouse small intestine. High magnification revealed a predominantly cytoplasmic immunolabeling, although, as expected by its molecular nature (nuclear phospho-protein) and function (cohesin complex / transcription factor),[16] RAD21-IR was also detectable in nuclei. No other cell types in the small intestinal *muscularis propria* displayed cytoplasmic RAD21-IR, including GFAP expressing glial cells, Kit+ ICC and PDGFRα-IR fibroblast-like cells. The specificity of the two anti-RAD21 antibodies was confirmed by a number experimental conditions and controls. First, both anti-RAD21 antibodies identified overlapping immunoreactive patterns, i.e. a selective subset of myenteric neurons (see below); secondly, omission of primary (or secondary) antibodies, substitution of the primary with secondary antibodies and pre-adsorption control did not yield any immunostaining; thirdly, experiments in which RAD21 was knocked-down by shRNA abolished RAD21-IR. Taken together these tests demonstrate the specificity of RAD21-IR and confirm neuronal expression. Based on this reliable immunolabeling, we investigated the intrinsic innervation of the human and mouse small intestine and identified RAD21 expression in myenteric ChAT-IR neurons, likely belonging to motor neurons / ascending interneurons.[17] By contrast, nNOS expressing myenteric neurons, mainly inhibitory motor neurons / descending interneurons, did not show RAD21-IR in either species. Our data provided the first analysis of RAD21 localization in the mammalian enteric nervous system and clearly showed that this cohesin complex protein is

expressed outside the nucleus of cholinergic neurons in a subset of ChAT-IR neurons. RAD21 is known to exert a variety of regulatory functions critical to cellular homeostasis,[18] thus our findings suggest a role for extra-nuclear RAD21 in maintenance and survival mechanisms of a subset of cholinergic neurons occurring in the healthy myenteric plexus.

Expression of RAD21 in the cytoplasm of cells has been previously associated with the translocation of a 64 KDa C-terminal fragment of the RAD21 protein from the nucleus following cleavage by caspases.[19] RAD21 contains a consensus caspase 3/7 cleavage site[20] and it has been proposed that RAD21 translocation is an early indicator of activation of caspase dependent apoptosis.[19] Both antibodies used in this study were directed against the C-terminal region of RAD21 and therefore would be expected to detect cleaved, cytoplasmic RAD21 if present. Recent studies in mice[21] and our own unpublished observations in human tissues found that a surprisingly high proportion (10–20%) of myenteric neurons express cleaved, active caspase-3 leading to the controversial suggestion that there is extensive ongoing apoptosis in the enteric nervous system. The proportion of caspase-3 positive neurons is much lower than the proportion of myenteric neurons that express cytoplasmic RAD21-IR (approximately 40%), thus it is unlikely that the presence of RAD21 in the cytoplasm is a marker for imminent cell death. However, the present study does indicate that RAD21 cleavage and translocation occurs preferentially in ChAT-positive, but not nNOS-positive, myenteric neurons possibly suggesting transient activation of caspase-3 activity in ChAT-positive neurons that does not always progress to cell death. In contrast, low caspase-3 activity or reduced RAD21 cleavage and translocation in nNOS-positive neurons could contribute to the sparing of these cells in healthy aging.[13]The impact of the identified loss-of-function mutation in RAD21, such as that reported to be associated with CIPO,[5] may be related to altered sensitivity of RAD21 to cleavage and inappropriate translocation of the protein leading to loss of some or all subtypes of myenteric neurons. This mechanism may be responsible for altered motor function in CIPO patients. However, the actual effect of the RAD21 p.Ala622Thr mutation is still to be clarified in an appropriate mouse model. It is worth noting that rad21 homozygous null mice are embryonic lethal.[22] *In vivo* studies in the rad21 morpholino zebrafish model showed a delayed intestinal transit along with a significant reduction of enteric neurons, a finding indicative of an oligoneuronal hypoganglionosis reminiscent of the neuropathic CIPO phenotype.[5] Our data indicate that RAD21 is not expressed by nitrergic inhibitory neurons, a functionally distinct subclass commonly targeted by damaging mechanisms taking place in experimental ($nNOS^{-/-}$ mice) and human enteric neuropathies, and detectable in early stages of achalasia or idiopathic gastroparesis.[23]

Finally, in order to understand whether RAD21 distribution in myenteric neurons was altered during development, we investigated the distribution and relative abundance of RAD21-IR neurons in neonatal mice. RAD21-IR neurons were quantitatively comparable in neonatal and young adult tissues, a finding implying that RAD21-IR was not altered by weaning in mice. However, we did not investigate aged mice and future research will establish whether aging affects cytoplasmic RAD21 expression and eventually enteric neuron function.

In conclusion, our data showed that RAD21 is expressed in a distinct subset of myenteric, i.e. cholinergic, neurons supplying the human and mouse small intestine. These findings, combined with the knowledge that RAD21 mutations occur in distinct CIPO cases, imply that the cholinergic subset may be the primary target in some patients with this pathological condition.

Acknowledgements

We thank Mr. Gary Stoltz, Mrs. Cheryl Bernard and Mrs. Kristy Zodrow as well as members of the Enteric NeuroScience Program at Mayo Clinic for their assistance and feedback on these studies as well as Mrs. Ann Schmeichel and Dr. Phillip A. Low for the generous gift of the mouse brain sections. The authors particularly thank Dr. Vanda Lennon for the generous gift of the human anti-HuC/D antibody.

Funding:

This work was supported by grants from University of Bologna (RFO funds) (to RDeG), the Telethon Foundation (GGP15171) of Italy (to RDeG and EB) and the 'Fondazione del Monte di Bologna e Ravenna', Bologna, Italy (to RDeG) and the NeuroGut Initial Training Network (607652 – ITN) part of the FP7 from the European Community (RDeG). US National Institutes of Health, P30DK084567, R01DK57061, and R01DK106011.

Funding bodies did not influence the content of this article.

Abbreviations:

CIPO	Chronic intestinal pseudo-obstruction
IR	Immunoreactivity
nNOS	neuronal nitric oxide synthase
NPY	Neuropeptide Y
ChAT	choline acetyl transferase
PDGFRα	Platelet-derived growth factor receptor-α
GFAP	glial fibrillary acid protein
ICC	interstitial cells of Cajal
PBS	phosphate buffered saline
DAPI	4,6-diamidino-phenylindole,dihydrochloride
GI	gastrointestinal
NT	non-targeting
MOI	multiplicity of infection

References

1. Xu H, Yan M, Patra J, et al. Enhanced RAD21 cohesin expression confers poor prognosis and resistance to chemotherapy in high grade luminal, basal and HER2 breast cancers. Breast Cancer Res. 2011; 21;13.

2. Guacci V Sister chromatid cohesion: the cohesin cleavage model does not ring true. Genes Cells. 2007;12:693–708. [PubMed: 17573771]

3. Faure AJ, Schmidt D, Watt S, et al. Cohesin regulates tissue-specific expression by stabilizing highly occupied cis-regulatory modules. Genome Res. 2012;22:2163–75. [PubMed: 22780989]

4. Biswas U, Hempel K, Llano E, Pendas A, Jessberger R. Distinct Roles of Meiosis-Specific Cohesin Complexes in Mammalian Spermatogenesis. PLoS Genet. 2016;12:e1006389. [PubMed: 27792785]

5. Bonora E, Bianco F, Cordeddu L, et al. Mutations in RAD21 disrupt regulation of APOB in patients with chronic intestinal pseudo-obstruction. Gastroenterology. 2015;148:771–782. [PubMed: 25575569]

6. Di Nardo G, Di Lorenzo C, Lauro A, et al. Chronic intestinal pseudo-obstruction in children and adults: diagnosis and therapeutic options. Neurogastroenterol Motil. 2017; 29.

7. Ohkubo H, Fuyuki A, Arimoto J, et al. Efficacy of percutaneous endoscopic gastro-jejunostomy (PEG-J) decompression therapy for patients with chronic intestinal pseudo-obstruction (CIPO). Neurogastroenterol Motil. 2017;e13127.

8. Deglincerti A, De Giorgio R, Cefle K, et al. A novel locus for syndromic chronic idiopathic intestinal pseudo-obstruction maps to chromosome 8q23-q24. Eur J Hum Genet. 2007;15:889–97. [PubMed: 17487221]

9. De Giorgio R, Barbara G, Furness JB, Tonini M. Novel therapeutic targets for enteric nervous system disorders. Trends Pharmacol Sci. 2007;28:473–81. [PubMed: 17764756]

10. Rao Meenakshi and Gershon Michael D.. The dynamic cycle of life in the enteric nervous system. Nat Rev Gastroenterol Hepatol. 2017;14:453–454. [PubMed: 28655880]

11. Furness JB The organisation of the autonomic nervous system: Peripheral connections. Auton Neurosci. 2006;130:1–5. [PubMed: 16798102]

12. Bianco F, Gibbons SJ, Bonora E, et al. Distribution of RAD21 immunoreactivity in mouse and human gut neurons. Neurogastroenterol Motil. Volume 29, Issue S2, page 30.

13. Bernard CE, Gibbons SJ, Gomez-Pinilla PJ, et al. Effect of age on the enteric nervous system of the human colon. Neurogastroenterol Motil. 2009;21:746–e46. [PubMed: 19220755]

14. Wouters MM, Gibbons SJ, Roeder JL, et al. Exogenous serotonin regulates proliferation of interstitial cells of Cajal in mouse jejunum through 5-HT2B receptors. Gastroenterology. 2007;133:897–906. [PubMed: 17854596]

15. Shute CC, Lewis PR. The ascending cholinergic reticular system: neocortical, olfactory and subcortical projections. Brain. 1967;90:497–520. [PubMed: 6058140]

16. Hauf S, Waizenegger IC, Peters JM. Cohesin cleavage by separase required for anaphase and cytokinesis in human cells. Science. 2001;293:1320–3. [PubMed: 11509732]

17. Bornstein JC, Costa M, Grider JR. Enteric motor and interneuronal circuits controlling motility. Neurogastroenterol Motil. 2004;16 Suppl 1:34–8. [PubMed: 15066002]

18. Mullenders J, Aranda-Orgilles B, Lhoumaud P, et al. Cohesin loss alters adult hematopoietic stem cell homeostasis, leading to myeloproliferative neoplasms. J Exp Med. 2015;212:1833–50. [PubMed: 26438359]

19. Pati D, Zhang N, Plon SE. Linking sister chromatid cohesion and apoptosis: role of Rad21. Mol Cell Biol. 2002;22:8267–77. [PubMed: 12417729]

20. Yang ZR. Prediction of caspase cleavage sites using Bayesian bio-basis function neural networks. Bioinformatics. 2005;21:1831–7. [PubMed: 15671118]

21. Kulkarni S, Micci MA, Leser J, et al. Adult enteric nervous system in health is maintained by a dynamic balance between neuronal apoptosis and neurogenesis. Proc Natl Acad Sci U S A. 2017;114.

22. Xu H, Balakrishnan K, Malaterre J, et al. Rad21-cohesin haploinsufficiency impedes DNA repair and enhances gastrointestinal radiosensitivity in mice. PLoS One. 2010;5:e12112. [PubMed: 20711430]

23. Grover M, Farrugia G, Lurken MS, et al. Cellular changes in diabetic and idiopathic gastroparesis. Gastroenterology. 2011;140:575–85.e8.

Key Points:

- This study focused on the characterization of RAD21-IR in enteric neurons of mice and human small intestine.
- The study showed that RAD21-IR is localized outside the nucleus in a subset of ChAT-IR neurons, but not in nNOS-IR neurons in human and mouse jejunum.
- These findings, combined with the knowledge that RAD21 mutations occur in distinct CIPO cases, imply that the cholinergic subset may be the primary target in some patients with this pathological condition.

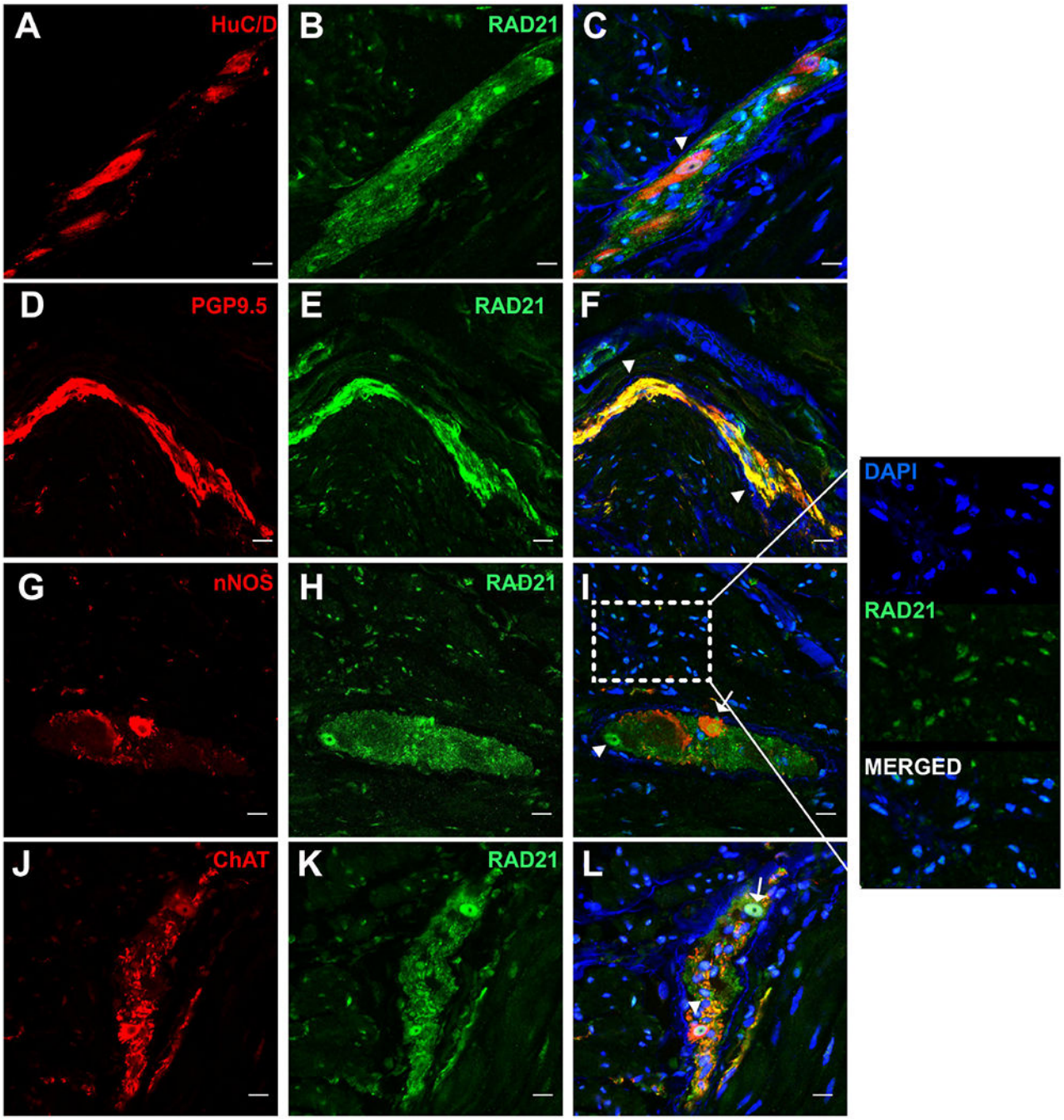

Figure 1. RAD21-IR in human small intestine.

RAD21-IR was distributed in neurons of the human small intestine. RAD21 was observed in cell bodies and nerve fibers (arrows) of a subset of enteric neurons identified by HuC/D-IR (**A-C** arrowhead) and PGP9.5 (**D-F** arrowheads). RAD21-IR was not found in the cytoplasm of nNOS-IR inhibitory neurons (**G-I** arrow indicates a nNOS-IR neuron with nuclear labeling). Arrowhead in panel I indicates a nNOS-negative neuron with RAD21-IR in the cytoplasm. Inset of panel I shows high resolution image of RAD21-IR in the nucleus of non-

neuronal cells. RAD21-IR also colocalized with ChAT in some neurons (**J-L** arrow). Scale bar 50 μm.

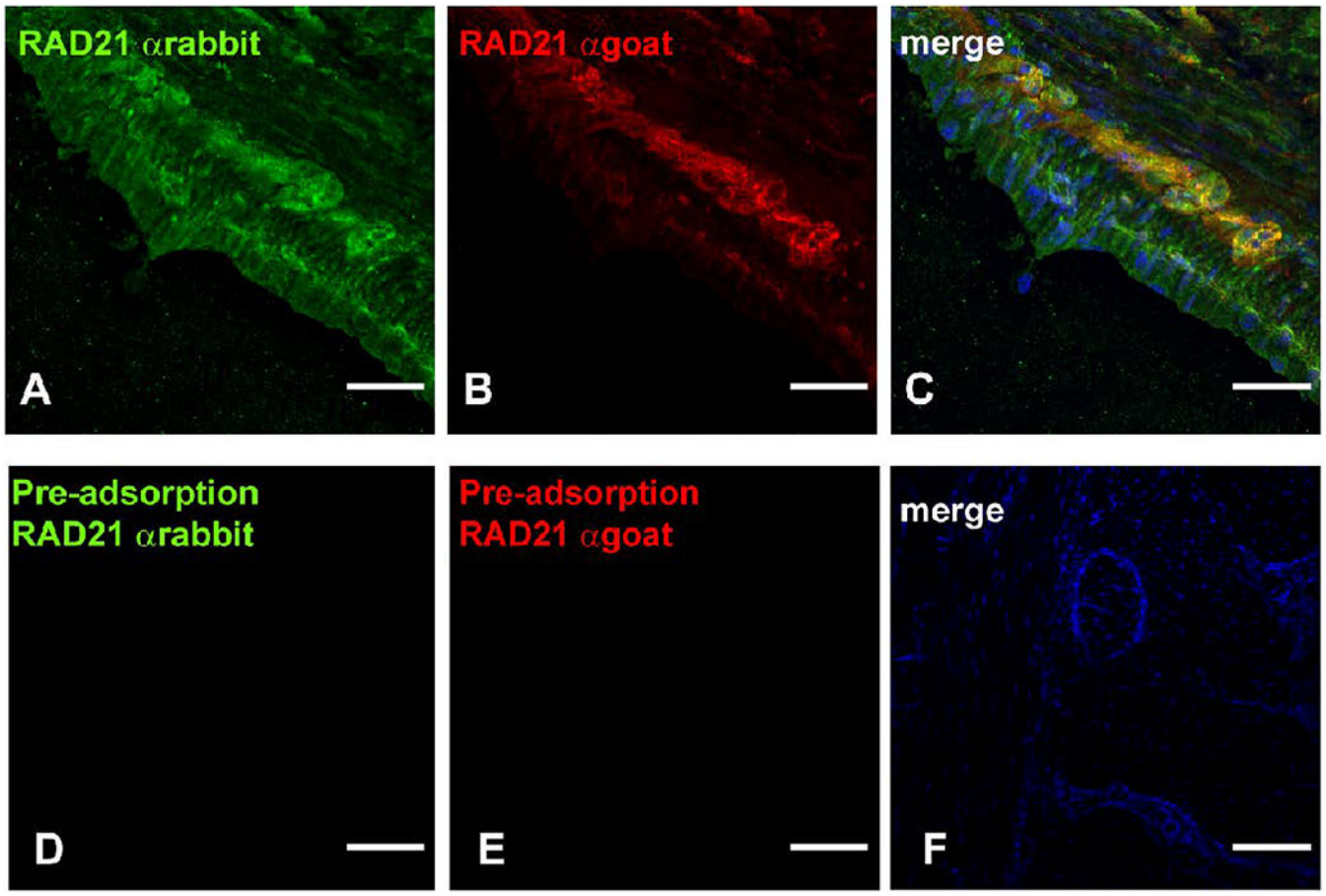

Figure 2. Double labeling with two different RAD21 primary antibodies.

Anti-rabbit in green (abcam ab992) (**A**) and anti-goat red (Santa Cruz sc54323) (**B**) anti-RAD21 antibodies labeled most brightly the same structures in BALB/C jejunum preparations. Colocalization is shown in yellow (**C**). Pre-adsorption of antibody with specific blocking peptide abolished the signal suggesting specificity of antibody used in this study (**D**-**F**). Scale bar 50 μm.

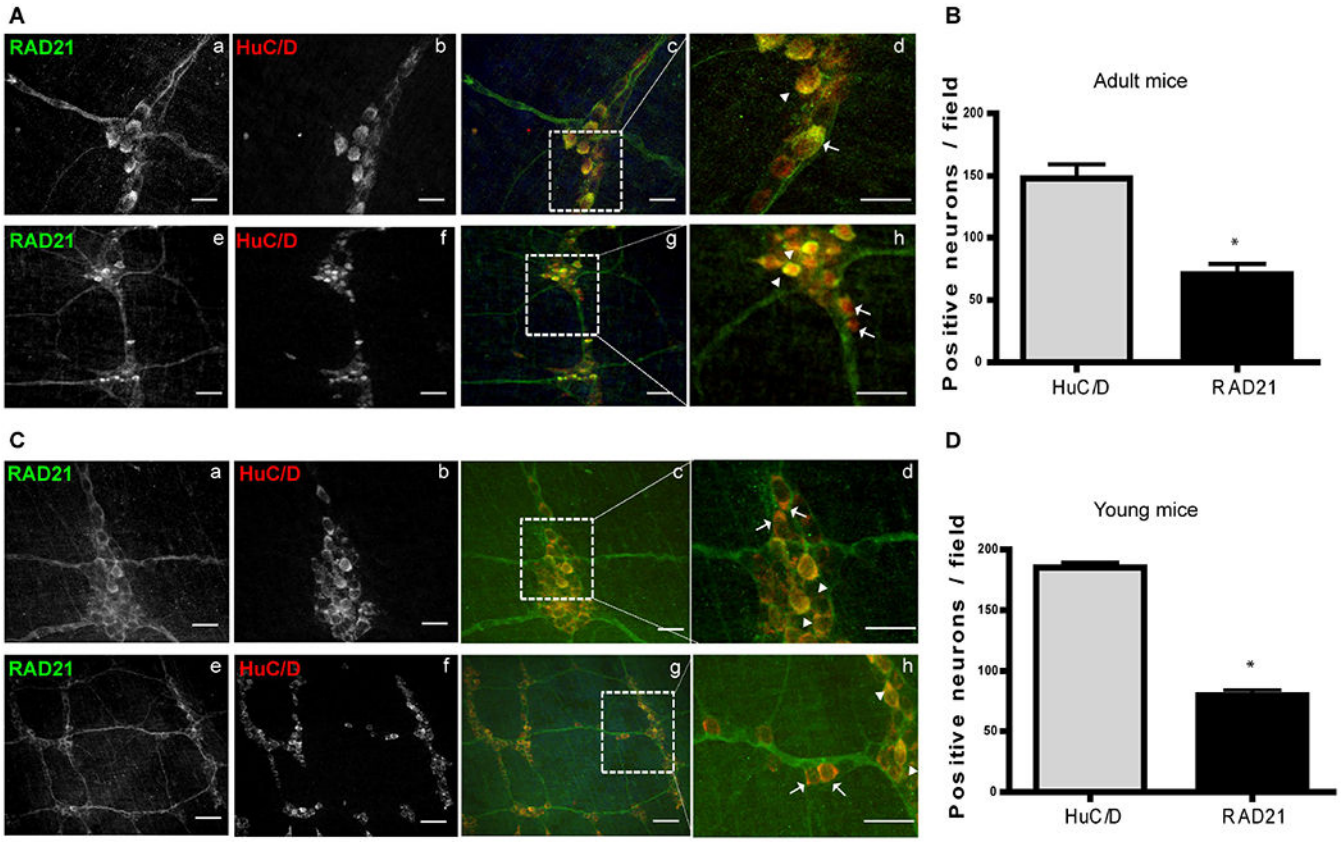

Figure 3. HuC/D, and RAD21 Immunolabeling in mouse jejunal whole mounts.

(A). Immunolabeling of RAD21 in whole mounts from adult mice. Within the myenteric plexus this pattern was found in 61.56±0.9 and 144.7±4.1 neurons/field for RAD21 and HuC/D, respectively (n=4, P <0.05, t-test). Scale bars: 10 and 50 μm for upper and lower panel, respectively. Photomicrographs in **A** (**d** and **h**) (merge) illustrate higher magnification insets of the indicated region (in white rectangle). Arrows indicates RAD21 single labeling and arrowheads indicates RAD21double labeling with HuC/D. Scale bar 20 μm. (**B)** Graphs showing the number of neurons per field of RAD21 and HuC/D expression in whole mounts preparations of adult BALB/C mice (n=4, P< 0.05). (**C)** Immunolabeling of RAD21 in whole mounts from young (4 to 10 day old) BALB/C mice. Within the myenteric plexus this pattern was found in 79.56±4.5 and 185.0±4.0 neurons/field for RAD21 and HuC/D, respectively (n=3 mice, P <0.05, t-test). Scale bars: 10 and 50 μm for upper and lower panel, respectively. Photomicrographs in **C** (**d** and **h**) (merge) illustrate higher magnification insets of the indicated region (in white rectangle). Arrows indicates RAD21 single labeling and arrowheads indicates RAD21double labeling with HuC/D. Scale bar 20 μm. (**D)** Graphs showing the number of neurons per field of RAD21 and HuC/D expression in whole mounts preparations of young BALB/C mice (n=3 mice, P<0.05).

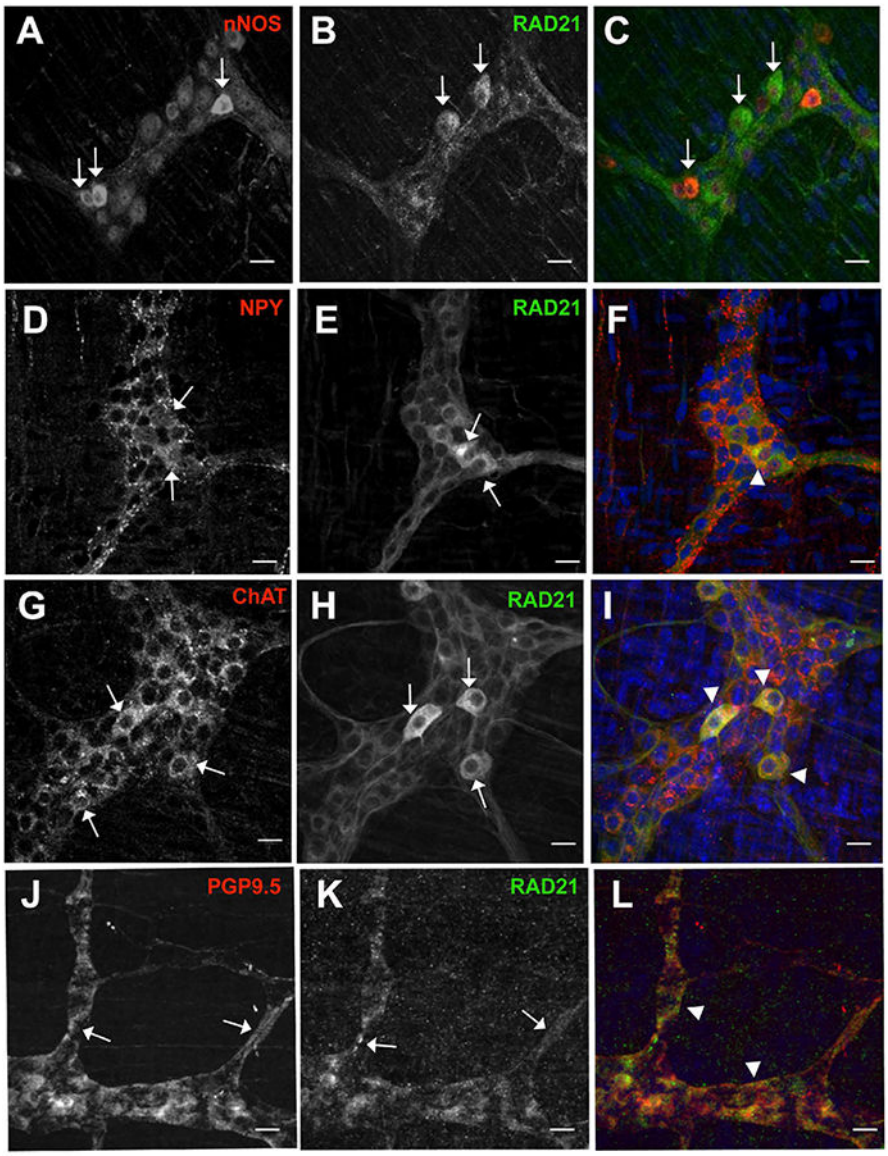

Figure 4. Double labeling of RAD21 with different neuronal markers.

RAD21-IR did not colocalize with neuronal nitric oxide synthase (nNOS) (**A-C** arrows). RAD21-IR was also present in neurons that were NPY positive (**D-F** arrowhead). RAD21-IR was present in a subset of ChAT positive neurons (**G-I** arrowhead). RAD21-IR colocalized with PGP9.5 in a subset of neuronal cell bodies and nerve fibers in the myenteric plexuses of mouse small intestine, (**J-L** arrowheads). Scale bar 50 μm.

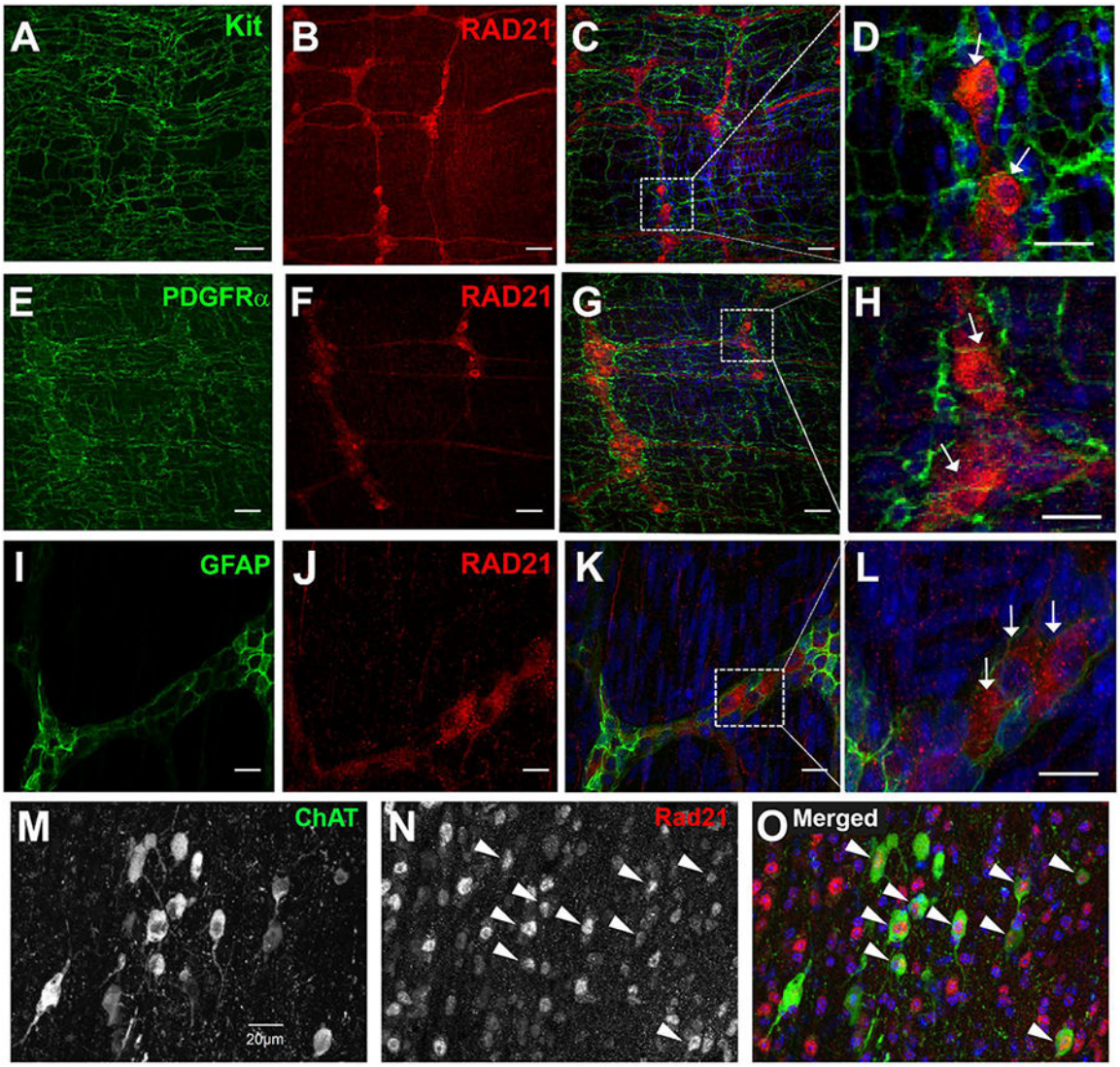

Figure 5. RAD21 did not colocalize with Kit (ICC), PDGFRα and GFAP and was not detected outside the nucleus of central neurons.

RAD21-IR was not detected in whole mounts preparations in the cytoplasm of interstitial cells of Cajal (ICC) with Kit (**A**-**D** arrows) and in fibroblast-like cells which were positive for PDGFRα (**E**-**H** arrows). RAD21 was not detectable in glial cells identified by GFAP (**I**-**L** arrows). Scale bar 50 μm. Photomicrographs in **D**, **H** and **L** (merge) illustrate higher magnification insets of the indicated region to show lack of co-localization. Scale bar 20 μm. Panels **M, N** and **O** show ChAT (green) and RAD21 (red) immunoreactivity in the basal forebrain of an adult mouse. Nuclei are labeled with DAPI (blue). RAD21 immunolabeling was detected in the nuclear region of approximately 50% of cells in the tissue and in the majority of ChAT positive neurons (arrowheads) had nuclear labeling for RAD21. RAD21 immunoreactivity was not detected outside the nucleus of any cells in this region of the brain.

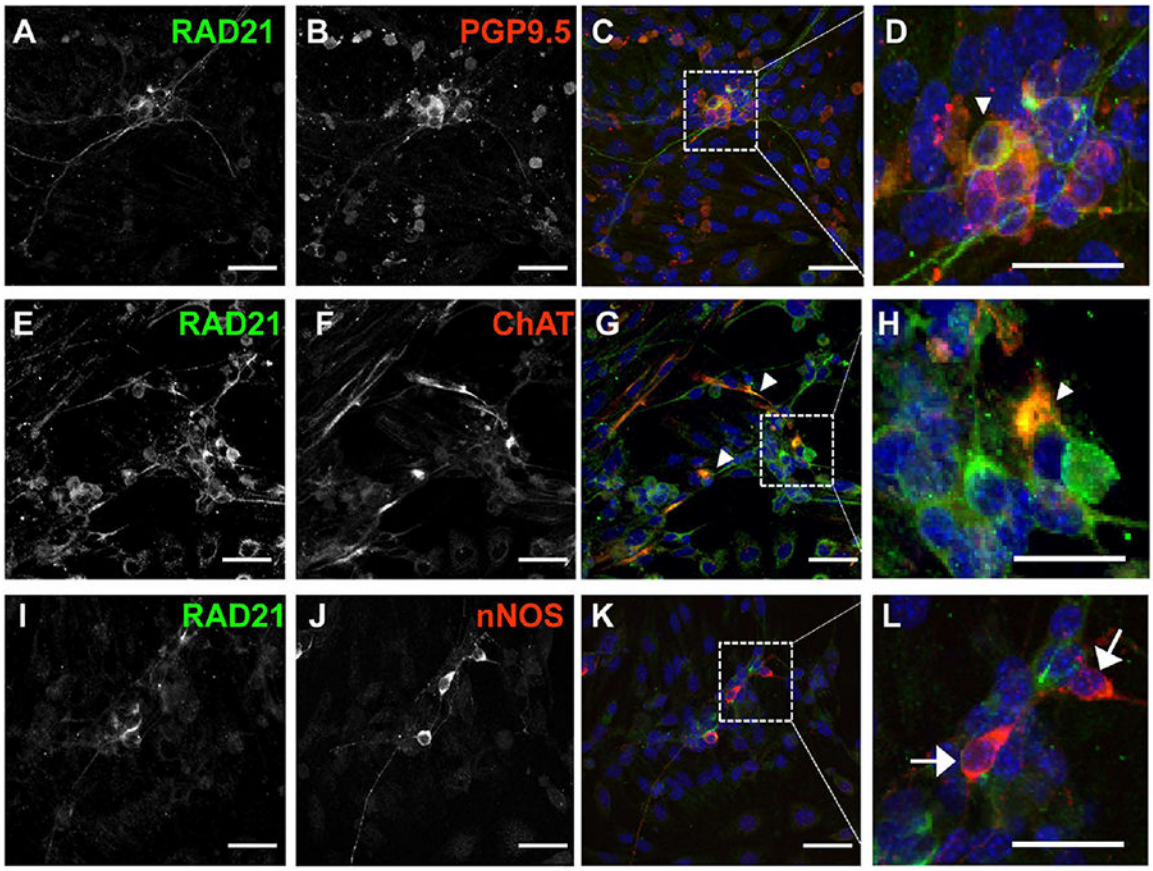

Figure 6. RAD21-IR in primary cultures from small intestine of BALB/C mice.

RAD21-IR in primary cultures from mice small intestine showed a similar distribution to that found in tissues. RAD21-IR was observed in cell bodies and nerve fibers of a subset of enteric neurons identified by PGP9.5-IR (A-D arrowhead). RAD21-IR also colocalized with ChAT in some neurons (E-H arrowhead), although none of the nNOS-IR neurons displayed RAD21 immunolabeling (I-L arrows). Scale bar 50 μm. Photomicrographs in D, H and L (merge) illustrate higher magnification insets of the indicated region. Scale bar 20 μm.

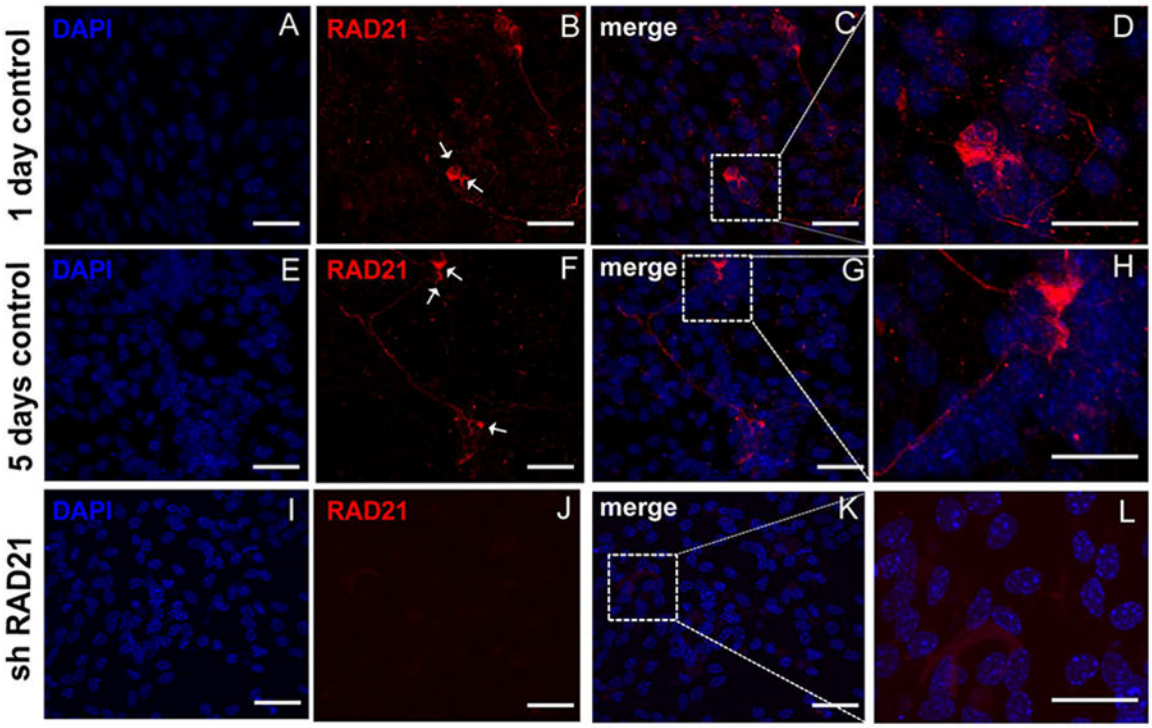

Figure 7. Selective silencing of RAD21-IR.

RAD21 knock down in 5 day old primary cultures. Note the absence of RAD21 expression in 5 day old primary cultures from the mouse jejunum after shRNA lentiviral particles treatment (**J**). No difference in the density or distribution of RAD21-IR was seen in untreated controls (**B**, **F** arrows) 1 or 5 days after seeding. Cells were immunolabelled for RAD21 at day 1 and 5 after seeding. Cells were treated with shRNA lentiviral particles at 24 hours after plating and grown for 4 days. Photomicrographs in **A**, **E** and **I** illustrate DAPI for cell nuclei staining. Photomicrographs **C**, **G** and **K** show merged images. Scale bar 50 μm. Photomicrographs in **D**, **H** and **L** (merge) illustrate higher magnification insets of the indicated region. Scale bar 20 μm.

Table 1.

List of primary and secondary antibodies used in this study.

Primary Antibodies	**Supplier**	**Host species**	**Titer**
RAD21	Abcam ab992	Rabbit	1 μg/mL
RAD21	Santa Cruz sc54323	Goat	1 μg/mL
HuC/D	Dr. Vanda Lennon *	Human	0.33 μg/mL
PGP9.5	Novus NB100–16403	Guinea pig	3.2 μg/mL
nNOS	Novus NB100–8580	Goat	0.33 μg/mL
ChAT	Millipore Ab144p	Goat	0.33 μg/mL
NPY	Chemicon AB1583	Sheep	0.5 μg/mL
PDGFRα	eBioscience #14140182	Rat	0.3 μg/mL
KIT CD117 (ACK2)	eBioscience #566	Rat	0.2 μg/mL
GFAP	Thermo Fisher #13-0300	Rat	0.5 μg/mL
Secondary Antibodies			
AlexaFluor 647 anti-goat IgG	Jackson (PA, USA) #705-605-147	Donkey	2.5 μg mL^{-1}
Cyanin-3 anti-goat IgG	Jackson (PA, USA) #705-165-147	Donkey	2.5 μg mL^{-1}
Cyanin-3 anti-mouse IgG	Jackson (PA, USA) #715-165-150	Donkey	2.5 μg mL^{-1}

Notes: ChAT, choline acetylcholinesterase; GFAP, glial fibrillary acidic protein; nNOS, neuronal nitric oxide synthase; NPY, neuropeptide Y;

* Fairman CL, Clagett-Dame M, Lennon VA, Epstein ML. Appearance of neurons in the developing chick gut. Dev Dyn. 1995 Oct;204(2):192–201.